Published in final edited form as:
Angew Chem Int Ed Engl. 2013 August 26; 52(35): 9238–9241. doi:10.1002/anie.201302137.

Driving Force for Oxygen Atom Transfer by Heme-Thiolate Enzymes**

Xiaoshi Wang,
Department of Chemistry, Princeton University, Princeton, NJ 08544, USA

Sebastian Peter,
Department of Bio- and Environmental Sciences, International Graduate School of Zittau, Zittau, D-02763, Germany

Dr. René Ullrich,
Department of Bio- and Environmental Sciences, International Graduate School of Zittau, Zittau, D-02763, Germany

Prof. Martibn Hofrichter, and
Department of Bio- and Environmental Sciences, International Graduate School of Zittau, Zittau, D-02763, Germany

Prof. John T. Groves
Department of Chemistry, Princeton University, Princeton, NJ 08544, USA, Fax: (+1) 609-258-0348, jtgroves@princeton.edu

Keywords

Compound I; Redox potential; Chloroperoxidase; Peroxygenase; AaeAPO; P450

The heme-thiolate peroxygenase from *Agrocybe aegerita* (*Aae*APO, EC 1.11.2.1) is a versatile biocatalyst and cytochrome P450 analog that catalyzes a variety of oxygenation reactions with high efficiency and selectivity.[1] Our recent kinetic characterization of *Aae*APO-catalyzed reactions has shown that *Aae*APO compound I is an oxo-Fe^{IV} porphyrin radical cation.[2] The reactivity of *Aae*APO-I toward a panel of substrates showed very fast C–H hydroxylation rates, similar to those of cytochrome P450 (CYP119-I),[3] and much faster than chloroperoxidase compound I (CPO-I).[4] Mechanistic probes have revealed a large hydrogen isotope effect for aliphatic C–H hydroxylation and rearranged products from the hydroxylation of norcarane.[1b] There is, however, very little information available regarding the thermodynamic properties of such highly reactive oxoiron species for any heme-thiolate proteins.

For hydrogen abstraction reactions, the redox potential of the oxidant is correlated with the rates of C–H activation.[5] Yet these values are often not accessible, especially for highly reactive oxidants. We have developed a method to measure redox potentials for oxometalloporphyrin model compounds that takes advantage of the rapid, reversible oxygen atom transfer between oxo-metal complexes and halide ions.[6] By using rapid-mixing stopped-flow spectroscopy, rate constants of both forward and reverse reactions are

**Support of this research by the National Institutes of Health (2R37 GM036298), the European Social Fund (080935557) and the European Union integrated project, Peroxicats (265397) are gratefully acknowledged.

Correspondence to: John T. Groves.

Supporting information for this article is available on the WWW under http://www.angewandte.org.

measured. Thus, the driving force of the unknown oxo-transfer redox couple (M^{n+2}=O/M^n) is obtained from the equilibrium constants for the reaction and the known potentials of the HOX/X^- couples. Using this method, the oxo-transfer driving force for several heme-enzyme model complexes have been measured, such as oxo-Mn^VTDMImP[6-7] and [oxo-Fe^{IV}-4-TMPyP]$^+$.[8]

Here, we describe measurements of the driving force for oxygen atom transfer by the heme-thiolate proteins *Aae*APO and CPO. We have found that oxo-transfer between *Aae*APO-I and chloride or bromide ions is fast *and reversible* (Scheme 1). The redox potential of the couple *Aae*APO-I/ferric-*Aae*APO has been obtained over a wide pH range from the rate constants of the forward and reverse reactions. Thus, the highly reactive *Aae*APO-I can be placed on an absolute energy scale and compared with those of CPO and HRP for the first time.

*Aae*APO-I was generated by the stoichiometric reaction of Fe^{III}-*Aae*APO with HOCl or HOBr and characterized by rapid mixing, stopped-flow spectroscopy. The UV/Vis spectral features of *Aae*APO-I generated with these hypohalous acids (Figure 1) are the same as those we recently reported for peroxyacid oxidations.[2] The Soret band of the ferric enzyme at 417 nm diminished over the first 50 ms after mixing while new absorbances characteristic of the formation of an oxo-Fe^{IV} porphyrin radical cation appeared at 361 and 694 nm. *Aae*APO-I subsequently decayed in a second, slower phase. SVD analysis of these transient spectra indicated that only two species were present in significant amounts during this transformation. The *Aae*APO-I formation rate was directly measured by monitoring the conversion of the ferric enzyme to oxo-Fe^{IV} radical cation. Binding of HOX to the heme iron is a rapid step and heterolytic FeO–X bond cleavage is rate-limiting.[2] Plotting the initial absorbance change at 417 nm against the HOX concentration afforded a linear relationship with no evidence of saturation. Second-order rate constants were obtained from the slopes (Figure S1).

The oxidation of *Aae*APO with HOCl or HOBr was examined over a range of pH as shown in Table 1. At pH 3.0, HOCl was used because HOBr is not stable at this pH. The slightly milder oxidant, HOBr, was used to generate *Aae*APO-I from pH 4.0-7.0 in good yield. We also measured the rates of CPO-I formation by the same method (Table S1). At pH 5.0, 4°C, the second-order rate constant for CPO-I formation was 2.3×10^6 $M^{-1}s^{-1}$, which is three-fold faster than that of *Aae*APO. Although *Aae*APO and CPO share ~30% sequence similarity, their active site environments, especially the acid-base residues, differ and CPO has a less accessible active site.[9]

We have found that *Aae*APO-I is also highly reactive toward halide ions. The formation of HOBr for the reaction of bromide ion with *Aae*APO-I was detected conveniently with the diagnostic indicator, phenol red.[11] The rapid tetra-bromination of phenol red was monitored by the characteristic red shift from 434 nm to 592 nm as shown in Scheme S1 and Figure S2. The oxygenation of bromide by CPO-I was found to be much slower than that of *Aae*APO-I at the same pH. (Figure S3) The reaction of chloride ion with *Aae*APO-I to afford hypochlorous acid was also found to occur with high efficiency but only under acidic conditions.

The kinetic behavior of halide ion oxygenation by *Aae*APO-I was then investigated by double-mixing, stopped-flow spectroscopy. At each selected pH, *Aae*APO-I was formed in the first push by mixing ferric enzyme with 3 eq of NaOBr or NaOCl. NaBr or NaCl solution was added in the second push after the peak amount of compound I had been achieved. Time-resolved, diode array spectra clearly showed the transformation of compound I back to the resting ferric state. Kinetic profiles were obtained by monitoring the

return of the Soret band of ferric *Aae*APO at 417 nm or ferric CPO at 399 nm and fitted to a single exponential equation (Figure S4). The observed pseudo-first order rate constants (k_{obs}) were found to vary linearly with [NaBr] or [NaCl]. The apparent second-order rate constants (k_{rev}) were calculated from the slopes and are summarized in Table 1 and Table S1. The pH dependence of log k_{rev} is plotted in Figure 2. A slope of -1.0 was obtained over the pH range studied for CPO, suggesting that a single proton is involved in the reaction. However, for *Aae*APO, the log k_{rev}/pH slope is only -0.3, suggesting that a protonation may not occur in the rate-determining step.

Taking advantage of this reversible and kinetically well-behaved oxygen atom transfer reaction (Scheme 1), we determined a set of equilibrium constants, K_{equi}, from the ratios of the measured forward and reverse rate constants. Since the redox potentials for the couples HOBr/Br^- and HOCl/Cl^- are known,[12] the corresponding oxygen atom transfer driving force for *Aae*APO-I could be calculated at each pH as shown in equations 1 and 2 (n=2, at 4°C).

$$\Delta E' = \frac{2.3RT}{nF} \lg K_{equi} \quad (1)$$

$$E'_{cpd-I/Fe^{III}} = E'_{HOX/X^-} - 0.0275 \lg K_{equi} \quad (2)$$

The derived compound I/ferric enzyme redox potentials for *Aae*APO and CPO are summarized in Table 1 and plotted in Figure 3. Fitting those points from pH 3.0 to 7.0 gave linear relationships with a slope of 0.048 for *Aae*APO and 0.056 for CPO, close to the theoretical value of 0.055 for the Nernst equation at 4 °C. This similarity supports a Nernst half-reaction involving two electrons and two protons as shown in Scheme 2.

As can be seen in Figure 3, the driving force for oxygen atom transfer for *Aae*APO-I and CPO-I are similar to that of HOBr and about 200 mV less than that of HOCl. *Aae*APO-I and CPO-I are both significantly more oxidizing than HRP-I, while *Aae*APO-I has slightly larger redox potentials than those of CPO-I over the entire pH range. Thus, the ordering of the redox potentials parallels the reactivity of these heme proteins. CPO-I reacts slowly with even weak C-H bonds,[4, 14] while HRP-I is barely able to oxidize C-H bonds at all. By contrast, *Aae*APO-I is highly reactive toward even very strong C-H bonds, so other active site factors may contribute to the greater facility of C-H hydroxylation than CPO. Similar halide oxidation data for cytochrome P450 is not available. However, by comparing the hydroxylation kinetics of *Aae*APO and CYP119 with similar aliphatic substrates,[3, 15] the redox properties of P450-I and *Aae*APO-I appear to lie on a similar scale.

What factors contribute to the significantly higher driving force for ferryl oxygen atom transfer by *Aae*APO-I and CPO-I reported here as compared to that of HRP-I? The axial ligand for *Aae*APO and CPO are both cysteine thiolate anions, while for HRP, it is a neutral, histidine nitrogen. The importance of hydrogen bonding to the cysteine thiolate of P450, CPO and NOS has been noted.[16] According to the Nernst half reaction (Scheme 2), the driving force for the conversion of $^{+\bullet}PorFe^{IV}=O$ to $PorFe^{III}$ via oxygen atom transfer has two contributions – the electron affinity and the *proton affinity* of the ferryl species. Although DFT calculations have indicated that the frontier orbitals of a heme-histidine compound I are at lower energy than the corresponding orbitals in heme-thiolate compound I,[17] the strong proton affinity of a thiolate bound compound I may provide a large driving force resulting in a higher net redox potentials and more reactive oxidants.[5k, 18] The intrinsic basicity of the ferryl oxygen in Cys-S-Fe^{IV}=O (compound II) in heme-thiolate

enzymes has been established.[19] Since Cys-S-Fe^{III}-OH_2 is the resting state, Cys-S-Fe^{III}-OH is also basic, thus contributing further to the two-electron, two-proton oxo-transfer redox couples determined here.

The *one-electron* redox potential of *Aae*APO-I, [E^o(I)], is a particularly important thermodynamic value because it is related to the bond strength [*D*(O–H)] and the pK_a, [pK_a (II)] of Fe^{IV}O–H in *Aae*APO-II (equation 3).[5a, 5b] For cases in which E^o(I) and pK_a(II) cannot be measured independently, equation 4 can be derived.[20] Since both E^o(I) and pK_a(II) have not been measured independently for any heme-enzyme, the two-electron, two-proton redox potential of *Aae*APO-I measured here may be a good first approximation of E^0(I). $E^{'}_{(\text{HRP-I/HRP-II})}$ and $E^{'}_{(\text{HRP-II/Ferric})}$ for HRP have been measured and were found to be similar (~0.95 V at pH 6.0).[13, 21] However, this result might be due to the fact that HRP-II is not basic and exists in the Fe^{IV}=O form in the functional pH range. The situation is different if we consider that *Aae*APO compound II is protonated.[19] For example, if *D*(O–H) is estimated to be in the range of 100 kcal/mol,[2, 22] the one-electron redox potential, $E^{'}_{(\text{cpd-I/cpd-II})}$, would be 1.4 V vs NHE at pH 7.0, significantly higher than the two-electron $E^{'}_{(\text{cpd-I/ferric})}$ potential of 1.2 V. Accordingly, from equation 5, the reduction potential of *Aae*APO-II ($E^{'}_{(\text{cpd-II/ferric})}$) can be estimated to be ~ 0.8 V. This unsymmetrical partitioning of the two redox steps may be an important factor in facilitating homolytic C-H bond scission by heme-thiolate proteins.

$$D(O-H)=nFE^{o}\,(I)+2.3RTpK_{a}\,(II)+57\pm 2 \quad (3)$$

$$D(O-H)=nFE^{'}_{cpd-I/cpd-II}+2.3RTpH+57\pm 2 \quad (4)$$

$$2E^{'}_{cpd-I/Fe^{III}}=E^{'}_{cpd-I/cpd-II}+E^{'}_{cpd-II/Fe^{III}} \quad (5)$$

In summary, the results show that chloride and bromide ions are readily oxidized by *Aae*APO-I to the corresponding hypohalous acids. The reversibility of this oxo-transfer reaction provides a rare opportunity to place ferryl oxo-transfers by the highly reactive heme-thiolate *Aae*APO-I and that of CPO-I on an absolute energy scale. With an estimated BDE for Fe^{IV}O–H in *Aae*APO-II we are able to obtain redox potentials of three redox couples interconnecting the resting ferric protein with its two oxidized forms, $^{+\bullet}$Por-Fe^{IV}=O and Fe^{IV}O–H.

Experimental Section

Reagents

Wild-type extracellular peroxygenase of *A. aegerita* (isoform II, pI 5.6, 46 kDa) was produced in bioreactors with a soybean-flour suspension as the growth substrate and purified as described previously.[2, 23] Kinetic experiments were performed as we have recently described.[2] Bromination of phenol red was detected by UV/Vis spectroscopy.[7a] At a chosen pH, 2 μl of 10 μM APO or CPO was added to a reaction mixture containing 20 μM of phenol red (sodium salt), 1mM H_2O_2 and 10 mM NaBr.

The oxidation of ferric enzyme with NaOBr or NaOCl was performed by stopped-flow spectroscopy with the single-mixing mode under the diode-array or single wavelength mode. The first syringe was filled with enzyme in a 100 mM buffer at a chosen pH. The second syringe was filled with the oxidant in slightly basic water solution. Equal volumes of the two reactants were mixed quickly. The halide ion oxidation reactions were performed using the

double-mixing mode. Native enzyme was mixed with an equal volume of oxidants (NaOCl or NaOBr) in the first push. After an aging time (optimized for each pH), the sodium halide solution was added in the second push. All concentrations reported are the final concentrations. All the experiments were carried out at 4 °C. The data were analyzed using Kinetic Studio from Hi-Tech.

Supplementary Material

Refer to Web version on PubMed Central for supplementary material.

References

1. a) Hofrichter M, Ullrich R, Pecyna MJ, Liers C, Lundell T. Appl Microbiol Biotechnol. 2010; 87:871–897. [PubMed: 20495915] b) Peter S, Kinne M, Wang X, Ullrich R, Kayser G, Groves JT, Hofrichter M. FEBS J. 2011; 278:3667–3675. [PubMed: 21812933] c) Ullrich R, Hofrichter M. FEBS Lett. 2005; 579:6247–6250. [PubMed: 16253244]
2. Wang X, Peter S, Kinne M, Hofrichter M, Groves JT. J Am Chem Soc. 2012; 134:12897–12900.
3. Rittle J, Green MT. Science. 2010; 330:933–937. [PubMed: 21071661]
4. Zhang R, Nagraj N, Lansakara DSP, Hager LP, Newcomb M. Org Lett. 2006; 8:2731–2734. [PubMed: 16774243]
5. a) Mayer JM. Acc Chem Res. 1998; 31:441–450.b) Bordwell FG, Cheng JP, Ji GZ, Satish AV, Zhang X. J Am Chem Soc. 1991; 113:9790–9795.c) Concepcion JJ, Jurss JW, Brennaman MK, Hoertz PG, Patrocinio AOT, Iha NYM, Templeton JL, Meyer TJ. Acc Chem Res. 2009; 42:1954–1965. [PubMed: 19817345] d) Meyer TJ, Huynh MHV, Thorp HH. Angew Chem. 2007; 119:5378–5399.Angew Chem Int Ed. 2007; 46:5284–5304.e) Mayer JM. Ann Rev Phys Chem. 2004; 55:363–390. [PubMed: 15117257] f) Cukier RI, Nocera DG. Ann Rev Phys Chem. 1998; 49:337–369. [PubMed: 9933908] g) Borovik AS. Chem Soc Rev. 2011; 40:1870–1874. [PubMed: 21365079] h) Warren JJ, Tronic TA, Mayer JM. Chem Rev. 2010; 110:6961–7001. [PubMed: 20925411] i) Gunay A, Theopold KH. Chem Rev. 2010; 110:1060–1081. [PubMed: 20143877] j) Waidmann CR, Miller AJM, Ng CWA, Scheuermann ML, Porter TR, Tronic TA, Mayer JM. Energy Env Sci. 2012; 5:7771–7780.k) Lai WZ, Li CS, Chen H, Shaik S. Angew Chem. 2012; 124:5652–5676.Angew Chem Int Ed. 2012; 51:5556–5578.
6. Jin N, Bourassa JL, Tizio SC, Groves JT. Angew Chem. 2000; 112:4007–4009.Angew Chem Int Ed. 2000; 39:3849–3851.
7. a) Lahaye D, Groves JT. J Inorg Biochem. 2007; 101:1786–1797. [PubMed: 17825916] b) Umile TP, Wang D, Groves JT. Inorg Chem. 2011; 50:10353–10362. [PubMed: 21936530] c) Umile TP, Groves JT. Angew Chem. 2011; 123:721–724.Angew Chem Int Ed. 2011; 50:695–698.
8. Bell, SR. PhD thesis. Princeton University (USA); 2010.
9. a) Pecyna MJ, Ullrich R, Bittner B, Clemens A, Scheibner K, Schubert R, Hofrichter M. Appl Microbiol Biotechnol. 2009; 84:885–897. [PubMed: 19434406] b) Sundaramoorthy M, Terner J, Poulos TL. Chem Biol. 1998; 5:461–473. [PubMed: 9751642]
10. Bard, AJ.; Parsons, R.; Jordan, J. Standard Potentials in Aqueous Solution. Marcel Dekker, Inc.; New York: 1985. p. 67-92.
11. a) Walker JV, Morey M, Carlsson H, Davidson A, Stucky GD, Butler A. J Am Chem Soc. 1997; 119:6921–6922.b) Totaro RM, Williams AM, Apella MC, Blesa MA, Baran EJ. J Chem Soc Dalton Trans. 2000:4403–4406.
12. Holm RH, Donahue JP. Polyhedron. 1993; 12:57–589.
13. Farhangrazi ZS, Fossett ME, Powers LS, Ellis WR Jr. Biochemistry. 1995; 34:2866–2871. [PubMed: 7893700]
14. Zaks A, Dodds DR. J Am Chem Soc. 1995; 117:10419–10424.
15. a) Su Z, Horner JH, Newcomb M. ChemBioChem. 2012; 13:2061–2064. [PubMed: 22890798] b) Davydov R, Dawson JH, Perera R, Hoffman BM. Biochemistry. 2013; 52:667–671. [PubMed: 23215047]

16. a) Mak PJ, Yang YT, Im S, Waskell LA, Kincaid JR. Angew Chem. 2012; 124:10549–10553.Angew Chem Int Ed. 2012; 51:10403–10407.b) Lang J, Santolini J, Couture M. Biochemistry. 2011; 50:10069–10081. [PubMed: 22023145] c) Galinato MGI, Spolitak T, Ballou DP, Lehnert N. Biochemistry. 2011; 50:1053–1069. [PubMed: 21158478]
17. a) Kumar D, De Visser SP, Sharma K, Derat E, Shaik S. J Biol Inorg Chem. 2005; 10:181–189. [PubMed: 15723206] b) Kumar D, Sastry GN, de Visser SP. J Phys Chem B. 2012; 116:718–730. [PubMed: 22132821]
18. a) Dey A, Jiang Y, Ortiz de Montellano R, Hodgson KO, Hedman B, Solomon EI. J Am Chem Soc. 2009; 131:7869–7878. [PubMed: 19438234] b) Takahashi A, Yamaki D, Ikemura K, Kurahashi T, Ogura T, Hada M, Fujii H. Inorg Chem. 2012; 51:7296–7305. [PubMed: 22716193] c) Hughes TF, Friesner RA. J Chem Theo Comp. 2012; 8:442–459.d) Isobe H, Yamaguchi K, Okumura M, Shimada J. J Phys Chem B. 2012; 116:4713–4730.
19. Green MT, Dawson JH, Gray HB. Science. 2004; 304:1653–1656. [PubMed: 15192224]
20. Wang D, Zhang M, Buhlmann P, Que L. J Am Chem Soc. 2010; 132:7638–7644. [PubMed: 20476758]
21. Hayashi Y, Yamazaki I. J Biol Chem. 1979; 254:9101–9106. [PubMed: 39073]
22. Bell SR, Groves JT. J Am Chem Soc. 2009; 131:9640–9641. [PubMed: 19552441]
23. Ullrich R, Nuske J, Scheibner K, Spantzel J, Hofrichter M. Appl Environ Microbiol. 2004; 70:4575–4581. [PubMed: 15294788]

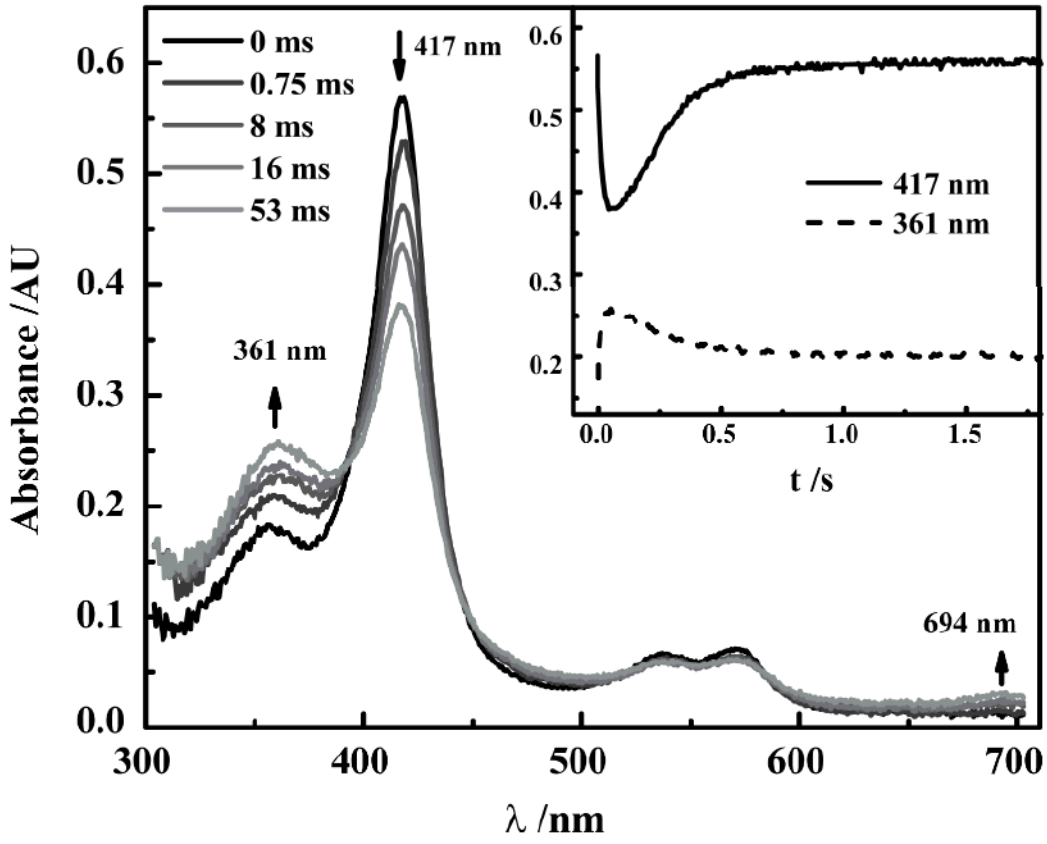

Figure 1.
UV/vis spectra observed upon 1:1 mixing of 5 μM *Aae*APO with 15 μM NaOBr at pH 5.0, 4°C. Inset: Time courses of data obtained at 417 nm (ferric *Aae*APO) and 361 nm (*Aae*APO-I).

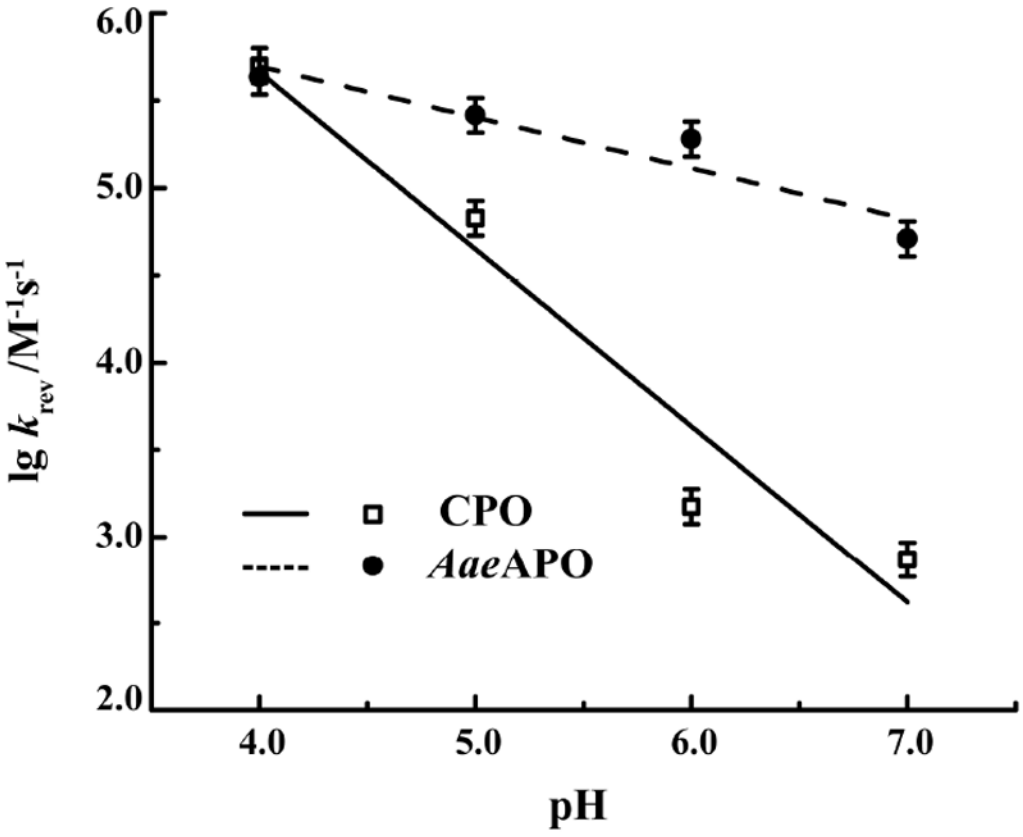

Figure 2.
Plots of log k_{rev} as a function of pH for oxo-transfer from *Aae*APO-I and CPO-I to bromide ion.

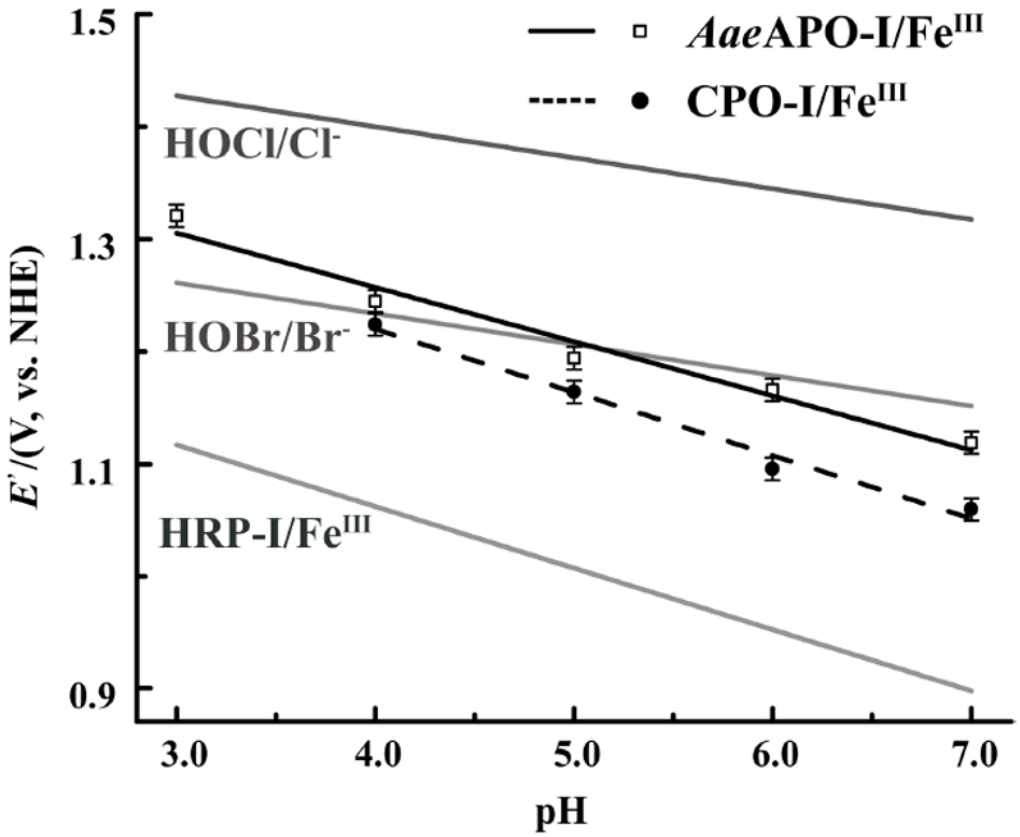

Figure 3.

Calculated redox potentials $E'_{(\text{cpd-I/ferric})}$ as a function of pH for *Aae*APO-I/Fe^{III} (open squares) and CPO-I/Fe^{III} (closed circles) at 4°C. Nernst equations for HRP-I/Fe^{III} [13], $HOBr/Br^-$ and $HOCl/Cl^-$ are plotted in gray for comparison.

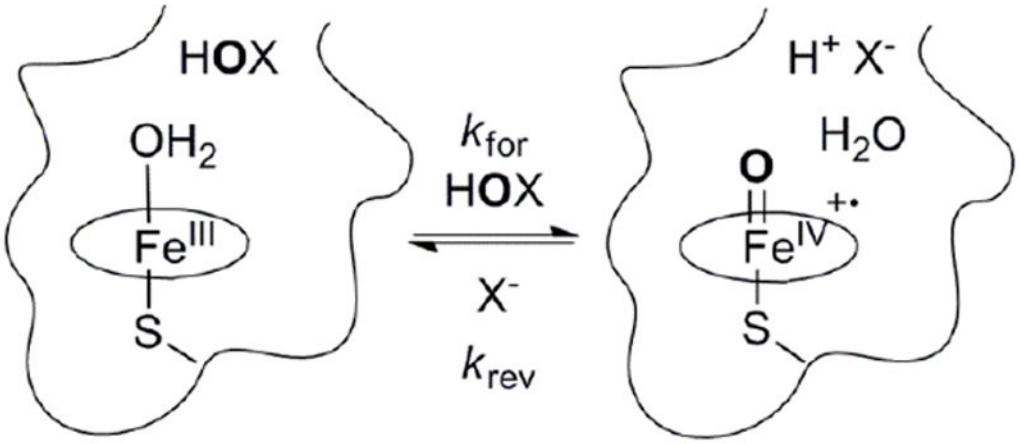

Scheme 1.
Reversible oxygen atom transfer between ferric *Aae*APO and HOBr or HOCl (k_{for}), and *Aae*APO-I with halide ions (k_{rev}).

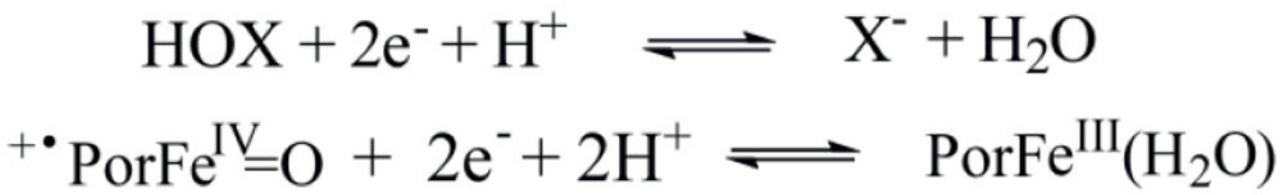

Scheme 2.
Nernst half-reactions for HOX and $^{+\bullet}$PorFe^{IV}=O.

Table 1

Data for oxygen atom transfer between halide ions and *Aae*APO-I as a function of pH.

pH	k_{for} ($M^{-1}s^{-1}$)	k_{rev} ($M^{-1}s^{-1}$)	K_{equi}	$E'_{(cpd\text{-}I/ferric)}$[a] [V, vs.NHE]
3.0	7.7×10^5	1.0×10^2	7680	1.32[b]
4.0	1.8×10^5	4.3×10^5	0.4	1.25
5.0	7.1×10^5	2.6×10^5	2.8	1.19
6.0	5.7×10^5	1.9×10^5	3.0	1.17
7.0	7.5×10^5	5.1×10^4	15	1.12

[a] based on the $HOBr/Br^-$ couple at 4°C except as noted.[10]

[b] based on the $HOCl/Cl^-$ couple at 4°C.[10]